Measuring Spectral Reflectance and 3D Shape Using Multi-primary Image Projector

Keita Hirai(✉), Ryosuke Nakahata, and Takahiko Horiuchi

Graduate School of Advanced Integration Science, Chiba University,
1-33, Yayoi-cho, Inage-ku, Chiba 263-8522, Japan
{hirai,horiuchi}@faculty.chiba-u.jp

Abstract. This paper presents a method to measure spectral reflectance and 3D shape of an object. For realizing these measurements, we applied a multi-primary image projector as a computational illumination system. This multi-primary image projector employs a light source which is programmable and can reproduce any spectral power distributions. In other words, the projector can reproduce 2D pattern projections with arbitrary spectra. In our actual measurements, we developed an imaging system by synchronizing the multi-primary image projector and a highspeed monochrome camera. First, the surface spectral reflectance of an object in a darkroom was obtained based on a finite-dimensional linear model of spectral reflectances. In the spectral reflectance measurements, nine basis images were projected and captured by the synchronized imaging system. Then spectral reflectance at each camera image coordinate was estimated from the captured nine images. Next, structured lights were projected for reconstructing 3D shape. We applied eight binary image projections and a conventional 3D shape reconstruction algorithm to our study. In summary, seventeen images were projected and captured for measuring spectral reflectance and 3D shape. The projection and capturing speed of the seventeen images is 0.085 s on the system specification. In the validation experiments, we could obtain spectral reflectance of X-rite ColorChecker with the average color difference ΔE^*_{ab} of approximately 4. We also confirmed that precise 3D shapes could be reconstructed by our method.

Keywords: Spectral reflectance · 3D shape · Fast measurement · Computational illumination system · Multi-primary image projector

1 Introduction

Measurements of object reflectance properties are important works in the research fields of computer vision, computer graphics, and color image analysis. Notably, color and geometric information are significant factors to determine object reflectance characteristics. For measuring these properties, various techniques have been proposed. In particular, computational illumination techniques and active lighting systems have been developed as useful tools to measure the reflectance properties.

A. Mansouri et al. (Eds.): ICISP 2016, LNCS 9680, pp. 137–147, 2016.
DOI: 10.1007/978-3-319-33618-3_15

Structured light projections have been applied to geometric calibrations and 3D shape measurements [1–3]. In these cases, a projector is generally used as a computational pattern illumination system. However, these researches mainly focus on the measurement of only geometric information. Almost related researches for measuring geometric information have not addressed accurate color measurements.

On the other hand, the techniques for measuring object color information have been also developed. Since measurements of surface spectral reflectance provide accurate color reproduction, various approaches based on active lighting systems have been recently proposed for measuring spectral reflectance [4–8]. In these previous systems, LEDs or spectral light sources are mainly used as active lighting systems. Then it is difficult for these lighting systems to implement 3D shape acquisitions based on the structured light projections.

In the research area of computer vision, a lot of methods based on inverse rendering techniques have been actively developed for recovering surface reflectance properties of both 3D shape and RGB color information [9–11]. In addition, several studies for digital archiving have measured 3D shape and spectral information simultaneously, because spectral information is significant for precise color recording in cultural heritage [12–17]. In these conventional methods, multi-band or multi-spectral cameras were used for acquiring spectral information. However, there are no projector-based computational illumination systems (active lighting systems) and techniques for rapidly measuring 3D shape and spectral reflectance.

In this research, therefore, we propose an imaging system to measure these reflectance properties at high speed. For achieving the goal, we apply a multi-primary image projector [18,19] to our measurement. The projector was developed to reproduce 2D image patterns with arbitrary spectra. This projector is a useful tool to project both structured light and spectrally-modulated illumination. Then we synchronized the projector with a highspeed monochrome camera for projecting and capturing computationally-illuminated images. In our measurements, first, surface spectral reflectance of an object in a darkroom is obtained based on the lighting technique with five spectral basis functions [5]. Then, binary stripe patterns [1] are projected for reconstructing 3D shape. Finally, we will discuss the measurement accuracies and time of spectral reflectance and 3D shape through our experiments. In addition, we apply the measured data to object relighting.

2 Multi-primary Image Projector

In this section, we briefly introduce the multi-primary image projector [18,19]. Figure 1 shows the configuration and projection principle of the projector. The image projection principle is practically the same as that used by digital light processing (DLP) projectors. The projected multi-primary images are produced by multiplexing time-sequential 2D pattern projections with various primary illuminant spectra. The time-sequential 2D image patterns correspond to the spatial weight distributions of each primary illuminant. Observers (cameras)

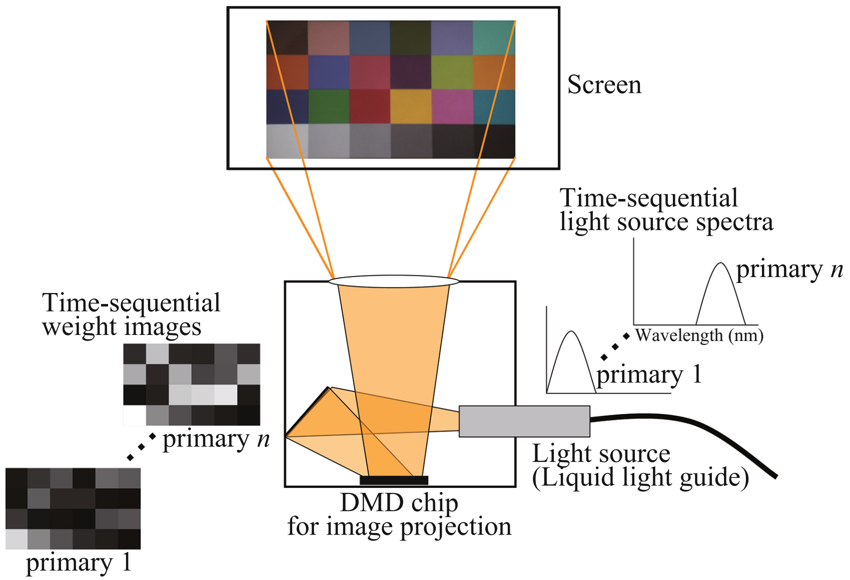

Fig. 1. Configuration and projection principle of the multi-primary image projector

perceive projected patterns that are expressed by spatially weighted SPDs of mixed multi-primary illuminants.

As shown in Fig. 1, the multi-primary image projector is mainly configured with a light source component and an image projection component. The light source component of the projector consists of Optronic Laboratories OL490, which is programmable using a computer. It is composed of a xenon lamp source, grating, a DMD chip, and a liquid light guide. The wavelength resolution is in the range of 380–780 nm. In this study, the sampling pitch for calculating the spectra is set at an interval of 10 nm. This sampling pitch is sufficient for practical spectral reflectance calculations. The image projection component of our prototype is based on a Texas Instruments DLP Lightcrafter. The original LED-based RGB primary colors were replaced with the above spectral light source. The present system uses a DMD chip with a resolution of 608×684 pixels for the image projection.

In summary, the grating and the DMD in the light source of the projector produces spectra, whereas the DMD in an image projection reproduces a monochromatic image with each light source spectrum. The light source and the image projection components are both controlled by a computer to project image sequences synchronously. A trigger signal is sent from the image projection component to the light source component. Table 1 shows the specifications of our multi-primary image projector. The increase of the number of time-sequential primaries means the decrease of light energy of each primary color. In other words, if it is necessary to reproduce high-intensity projection and reduce imaging noises, the projection speed of each primary should be lower.

Table 1. Typical examples of the multi-primary image projector specifications

Image bit depth	Number of primaries	Frames/sec
1 bit	1 primary	4000 fps
1 bit	20 primaries	200 fps
4 bits	1 primary	360 fps
6 bits	1 primary	240 fps
8 bits	1 primary	120 fps
8 bits	4 primaries	30 fps
8 bits	6 primaries	20 fps

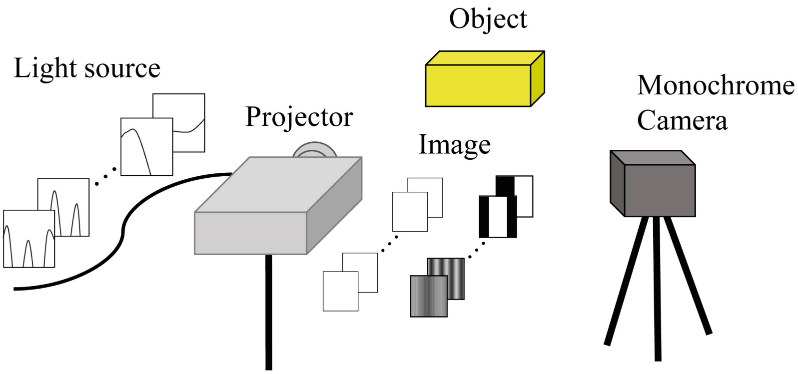

Fig. 2. Overview of our measurement system

3 Measurement System and Algorithms

3.1 Measurement System

Figure 2 shows the overview of our measurement system using the multi-primary image projector and a highspeed monochrome camera. The projector and camera are completely synchronized by a trigger signal. Thus there are no flicker effects between projections and captures in our measurements. As shown in Fig. 3, the projector reproduces nine basis images for estimating spectral reflectance (see Sect. 3.2) and eight binary stripe patterns for reconstructing 3D shape (see Sect. 3.3). Then, we project seventeen images in total for the measurement.

The highspeed monochrome camera is EPIX SV642M (resolution: 640×476 pixels, quantization bit depth: 10 bits, frame rate: 200 fps). In an ideal case, we project binary images (maximum projection speed is 4000 fps as shown in Table 1) and capture them (maximum capturing speed is 200 fps). Then, the projection and capturing speed of the seventeen images is 0.085 s (17 images divided by 200 fps) on the system specification. However, in our actual measurements, for increasing illumination intensities and reducing imaging noises,

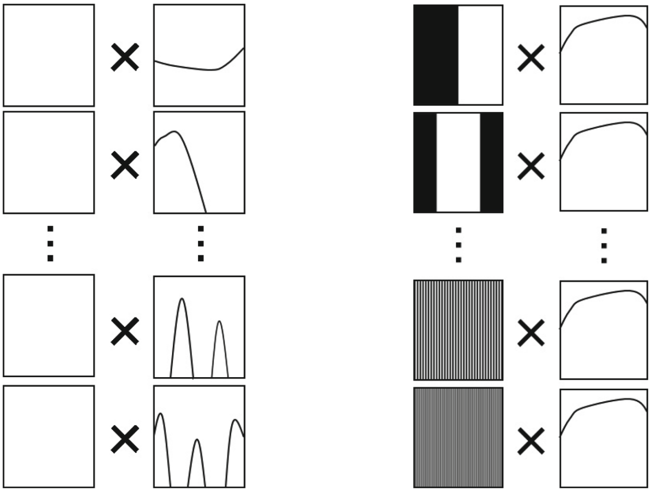

Fig. 3. Projected images: (left) nine basis images for spectral reflectance estimation (nine spectral basis light sources with a white image), and (right) eight stripe images for 3D shape reconstruction (eight stripe pattern images with a white light source).

the practical projection and capturing speed is later than the theoretical one (see also experimental discussions in Sect. 4).

3.2 Estimating Spectral Reflecntance

We use a set of orthonormal basis functions $\psi_m(\lambda)$ to represent surface spectral reflectance [5]. Surface spectral reflectance $S(\lambda)$ can be expressed as

$$S(\lambda) = \sum_{m=1}^{M} w_m \psi_m(\lambda) \quad (m = 1, 2, \ldots, M), \tag{1}$$

where M is the number of the orthonormal basis functions, w_m are the weights of the functions and λ indicates the wavelength. In this study, we selected five spectral basis functions, i.e., $M = 5$. The basis functions were computed by the principal component analysis (PCA) of a spectral reflectance database with 507 samples. Now, if we irradiate an object surface with spectrum $E_m(\lambda)$ of the orthonormal basis functions divided by the camera sensitivity $R(\lambda)$, the camera output O_m can be modeled as

$$\begin{aligned} O_m &= \int E_m(\lambda) R(\lambda) S(\lambda) d\lambda \\ &= \int (\psi_m(\lambda)/R(\lambda)) R(\lambda) \sum_{m=1}^{M} w_m \psi_m(\lambda) d\lambda \\ &= w_m. \end{aligned} \tag{2}$$

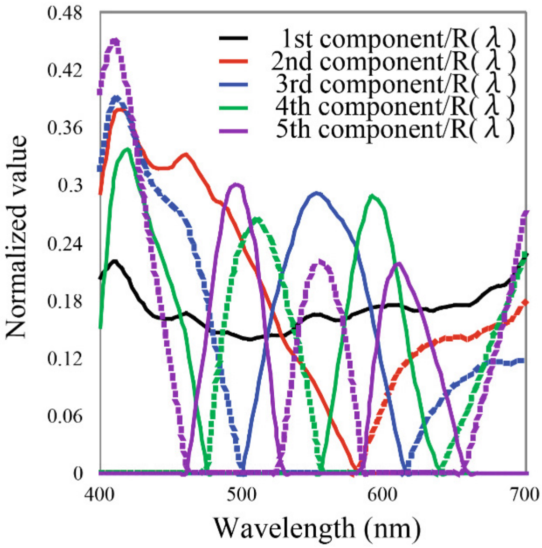

Fig. 4. Projected waveforms of orthonormal basis functions. The waveforms divided by the camera sensitivity are decomposed into positive and negative orthogonal basis (Color figure online).

As shown in Eq. (2), we can directly obtain the weights w_m from the camera outputs which are obtained by the projections based on the orthonormal basis functions. In actual case, we were unable to irradiate an object surface with the spectral basis functions based on PCA, because the orthonormal basis functions include negative values. In this study, we decompose the orthonormal basis functions into positive and negative functions. Then the absolute values of the decomposed negative functions are used as the projected illumination. Finally we estimate surface spectral reflectance using following values:

$$\psi_m(\lambda) = \psi_m^+(\lambda) - \psi_m^-(\lambda), \quad w_m = O_m^+ - O_m^-. \tag{3}$$

Figure 4 shows the projected spectra designed for estimating spectral reflectance. The figure shows the waveforms of nine orthonormal basis functions with the negative values inverted and which are divided by the camera spectral sensitivity $R(\lambda)$. The solid lines are the waveforms that are calculated by dividing the positive original orthonormal bases by the camera spectral sensitivity, and a dashed lines are the waveforms that are obtained by dividing the reversed negative components by the camera sensitivity. The second to fifth principle components include negative values and require illumination of two sources each. Then, nine waveforms are projected for spectral reflectance estimation.

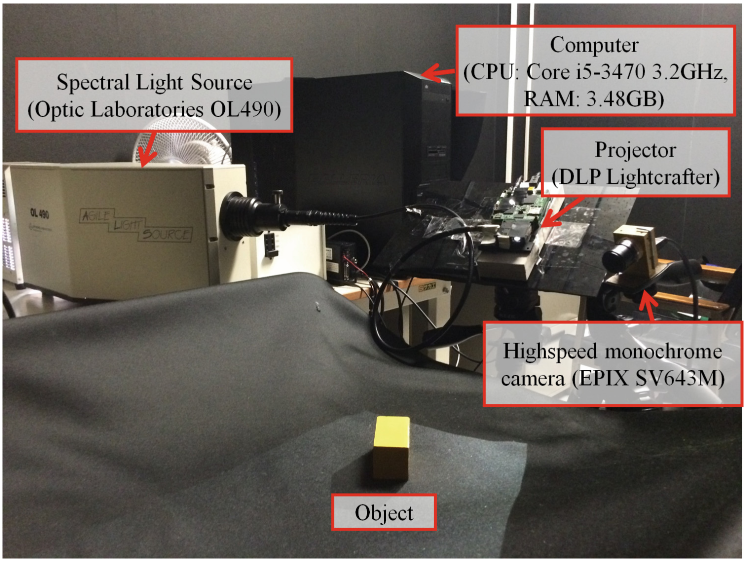

Fig. 5. Experimental setup for measuring spectral reflectance and 3D shape

3.3 Reconstructing 3D Shape

We apply the binary pattern image projection technique [1] to our 3D shape reconstruction. In general, N image patterns can express 2^N stripes. As shown in Fig. 3(b), we project eight pattern images ($N = 8$). Once binary image patterns are projected onto an object, there are 256 (2^8) unique areas coded with unique stripes. The 3D coordinates (X, Y, Z) can be computed for all 256 points along each horizontal line. Finally, 3D shape of an object can be reconstructed based on a triangulation principle and preliminary geometric calibrations.

4 Experimental Results and Discussions

Figure 5 shows our experimental setup for measuring spectral reflectance and 3D shape of an object. The actual experiments were conducted in a dark room. As the preliminary geometric calibration for precise 3D shape reconstruction, we used 75 reference points of a cube.

For validating the spectral reflectance estimation, we used an X-Rite Mini ColorChecker. Figure 6 shows examples which color differences ΔE^*_{ab} are the minimum and maximum in the ColorChecker. The average root mean square error (RMSE), goodness-of-fit coefficient (GFC) [20] and color difference ΔE^*_{ab} of 24 colors are 0.033, 0.9930 and 4.37, respectively. Compared with a conventional work [8], our system can estimate spectral reflectance with sufficient accuracy.

For verifying the accuracy of the 3D shape reconstruction, we used several single-color objects. Figure 7 shows an example of a measured object

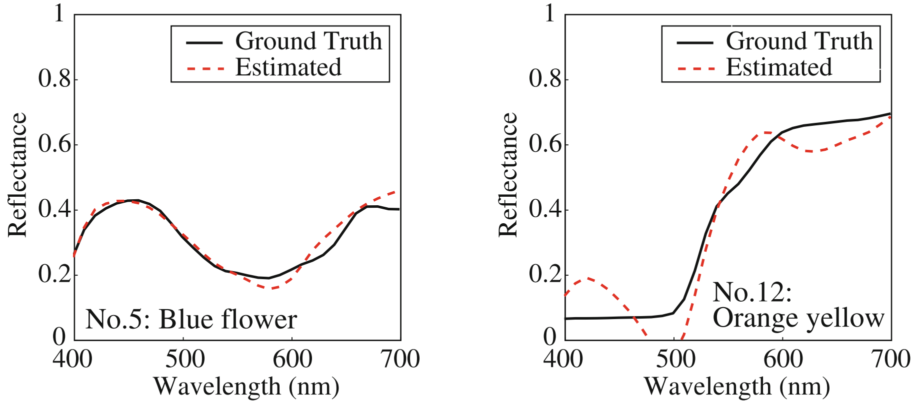

Fig. 6. Estimated spectral reflectances: (left) reflectance of ColorChecker No.5 which is estimated with the minimum color difference ($RMSE = 0.024$, $GFC = 0.9978$, $\Delta E^*_{ab} = 1.25$), and (right) reflectance of ColorChecker No.12 which is estimated with the maximum color difference ($RMSE = 0.074$, $GFC = 0.9872$, $\Delta E^*_{ab} = 10.96$).

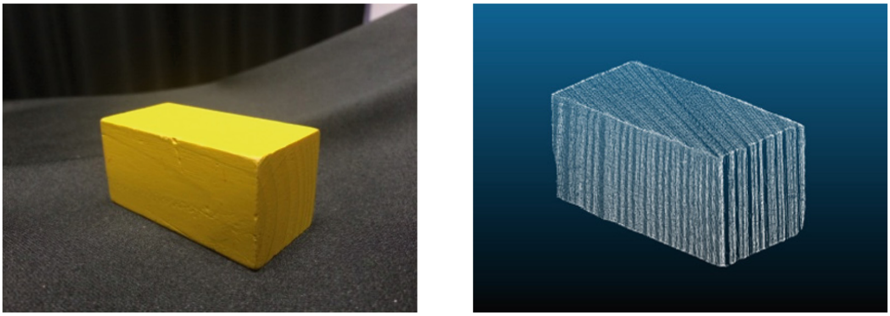

Fig. 7. Measured object (yellow cuboid made of wood) and its 3D mesh representation (Color figure online)

(yellow cuboid made of wood). As shown in the mesh data of Fig. 7, the 3D shape seems to be well reconstructed. We also confirmed that our 3D shape reconstruction had good accuracy compared with a commercial RGB-D camera (Kinect v2).

In the measurement of the spectral reflectance and 3D shape of the yellow object, the projection and capturing speed of seventeen images was 0.425 s. In our current system, if we need to measure more accurate data, making the measurement speed slower is required for achieving higher-intensity projections and less imaging noises. Similarly, we can make the measurement speed faster when we don't require such measurement accuracies. For achieving more rapid and accurate measurements, it is necessary to use a high-intensity light source and a high-sensitivity camera.

Fig. 8. Relighted objects: (left) relighting by illuminant A located at left-side position, and (right) relighting by illuminant D65 located at right-side position.

Finally, we applied the measured data to the object relighting (Fig. 8). The image rendering based on spectral calculations was implemented on PBRT (physically based rendering system). Through a brief experiment, we confirmed that the appearance of the rendered image is similar to the one of actual objects under the illuminations.

5 Conclusions

In this study, we have developed an imaging system for measuring spectral reflectance and 3D shape of scene objects. In our measurement system, we used the multi-primary image projector for computational spatial-spectral pattern projections. The average color difference ΔE^*_{ab} between the measured reflectances and the ground truths of X-Rite Mini ColorChecker was 4.37. We also reconstructed proper 3D shapes of colored objects. Finally, we demonstrated the object relighting using the measured spectral reflectances and 3D shapes.

In the experiments in this paper, we used single-color diffuse objects. For further discussion, we will conduct more experiments using objects with non-diffuse reflectance (specular, transmittance, etc.) and scenes with multiple textured objects. In addition, as discussed in Sect. 4, one problem with our system is the low projection and capturing speed in practical measurements. This is due to the avoidance of noisy image capturing caused by the low illumination intensities. This could be improved in the future by using a high-power light source and a noiseless camera. The improved system will provide rapid and accurate measurements. Finally, as a further future work, we would like to develop a technique for a real-time relighting system.

Acknowledgments. This work was partially supported by JSPS Grant-in-Aid for Scientific Research (C) (Grant Number 25330184).

References

1. Geng, J., Waterman, M.S.: Structured-light 3D surface imaging: a tutorial. Adv. Opt. Photonics **3**(2), 128–160 (2011)
2. Salvi, J., Pages, J., Batlle, J.: Pattern codification strategies in structured light systems. Pattern Recogn. **34**(4), 827–849 (2004)
3. Bimber, O., Raskar, R.: Spatial Augmented Reality: Merging Real and Virtual Worlds. A.K. Peters/CRC Press, Natick (2005)
4. Park, J.I., Lee, M.H., Grossberg, M.D., Nayar, S.K.: Multispectral imaging using multiplexed illumination. In: IEEE 11th International Conference on Computer Vision (ICCV), pp. 1–8 (2007)
5. Tominaga, S., Horiuchi, T.: Spectral imaging by synchronizing capture and illumination. J. Opt. Soc. Am. A **29**(9), 1764–1775 (2012)
6. Hirai, K., Tanimoto, T., Yamamoto, K., Horiuchi, T., Tominaga, S.: An LED-based spectral imaging system for surface reflectance and normal estimation. In: The 9th International Conference on Signal-Image Technology & Internet-Based Systems (SITIS), pp. 441–447 (2013)
7. Han, S., Sato, I., Okabe, T., Sato, Y.: Fast spectral reflectance recovery using DLP projector. Int. J. Comput. Vis. **110**(2), 172–184 (2014)
8. Nakahata, R., Hirai, K., Horiuchi, T., Tominaga, S.: Development of a dynamic relighting system for moving planar objects with unknown reflectance. In: Trémeau, A., Schettini, R., Tominaga, S. (eds.) CCIW 2015. LNCS, vol. 9016, pp. 81–90. Springer, Heidelberg (2015)
9. Sato, Y., Wheeler, M.D., Ikeuchi, K.: Object shape and reflectance modeling from observation. In: SIGGRAPH, pp. 379–387 (1997)
10. Oxholm, G., Nishino, K.: Shape and reflectance from natural illumination. In: Fitzgibbon, A., Lazebnik, S., Perona, P., Sato, Y., Schmid, C. (eds.) ECCV 2012, Part I. LNCS, vol. 7572, pp. 528–541. Springer, Heidelberg (2012)
11. Patow, G., Pueyo, X.: A survey of inverse rendering problems. Comput. Graph. Forum **22**(4), 663–687 (2003)
12. Tonsho, K., Akao, Y., Tsumura, N., Miyake, Y.: Development of goniophotometric imaging system for recording reflectance spectra of 3D objects. In: Proceedings of SPIE, vol. 4663, pp. 370–378 (2001)
13. Manabe, Y., Parkkinen, J., Jaaskelainen, T., Chihara, K.: Three dimensional measurement using color structured patterns and imaging spectrograph. In: 16th International Conference on Pattern Recognition (ICPR), pp. 649–652 (2002)
14. Tominaga, S., Tanaka, N.: Spectral image acquisition, analysis, and rendering for art paintings. J. Electron. Imaging **17**(4), 043022:1–043022:13 (2008)
15. Mansouri, A., Lathuiliere, A., Marzani, F.S., Voisin, Y., Gouton, P.: Toward a 3D multispectral scanner: an application to multimedia. IEEE MultiMedia **14**(1), 40–47 (2007)
16. Chane, C.S., Schutze, R., Boochs, F., Marzani, F.S.: Registration of 3D and multispectral data for the study of cultural heritage surfaces. Sensors **13**(1), 1004–1020 (2013)
17. Sitnik, R., Krzesłowski, J., Maczkowski, G.: Archiving shape and appearance of cultural heritage objects using structured light projection and multispectral imaging. Opt. Eng. **51**(2), 021115:1–021115:8 (2012)
18. Hirai, K., Irie, D., Horiuchi, T.: Multi-primary image projector using programmable spectral light source. J. Soc. Inf. Display (2016). doi:10.1002/jsid.422

19. Hirai, K., Irie, D., Horiuchi, T.: Photometric and geometric measurements based on multi-primary image projector. In: Colour and Visual Computing Symposium (CVCS), pp. 1–5 (2015)
20. Romero, J., García-Beltrán, A., Hernández-Andrés, J.: Linear basis for representation of natural and artificial illuminants. J. Opt. Soc. Am. A **14**(5), 1007–1014 (1997)